Journal Name

ARTICLE TYPE

Cite this: DOI: 10.1039/xxxxxxxxxx

X-ray reflectivity reveals ionic structure at liquid crystal - aqueous interfaces†

James E. Hallett,[a,b,c] Dominic Hayward,[a,b,c] Thomas Arnold,[d] Paul Bartlett[b] and Robert M. Richardson[a]

Received Date
Accepted Date

DOI: 10.1039/xxxxxxxxxx

www.rsc.org/journalname

Here X-ray reflectivity has been used to determine the structure of liquid crystal monolayers for different cyanobiphenyl homologues supported on aqueous solutions of two different salt species. Sodium iodide induces homeotropic ordering for all of the monolayer forming liquid crystal homologues studied here, and forms a Stern layer of iodide ions at the liquid crystal cyano headgroup, similar to the case of lipids or surfactants supported on electrolyte solutions. The liquid crystal headgroups were also found to penetrate into the water surface when binding with iodide ions. Sodium bromide, however, does not form the same localisation of ions close to a liquid crystal monolayer, and instead appears to produce no noticeable change in the scattering length density of the liquid crystal monolayer compared to pure water. However, on further compression the X-ray reflectivity dramatically changes, revealing the emergence of the so-called "trilayer" structure for 5CB and 8CB. This transition occurs at a lower areal density for sodium bromide than for pure water, and unlike for the uncompressed film, a layer of bromide ions was found at the trilayer-water interface.

1 Introduction

The local director (preferred molecular orientation) of a nematic liquid crystal phase can be controlled via external fields (e.g. magnetic or electric) or via surface structuring (e.g. steric brush layer, rubbed polymer layer). While external fields act on the nematic bulk, surface structuring reorients the first few layers of liquid crystal at a surface - but such is the strong elastic interaction of the nematic director, this preferential orientation can persist through the whole liquid crystal sample[1]. One of the most widely studied families of thermotropic liquid crystal are the *n*-cyanobiphenyls (*n*CB). The structures of some cyanobiphenyl homologues are shown in figure 1. Although not necessarily an intended consequence of their design, the *n*CB family are amphiphilic: the combination of a polar cyano headgroup and a hydrophobic alkyl tail of various lengths imparts this property. In mixtures of liquid crystal and water they form emulsions, or can form a monolayer when spread on water[2]. One use of these properties is that, as amphiphiles, their interfacial behaviour can be tuned by solutes in the aqueous phase. As liquid crystals, changes in the surface anchoring can result in reorientations that persist through the nematic bulk, producing an optical signal when viewed through crossed polarisers. These coupled mechanisms result in a unique system for the detection or measurement of chemicals in solution. Several recent papers have already demonstrated the high sensitivity of liquid crystal-water interfaces in either planar or droplet geometries[3], for the detection of agents such as bacterial endotoxin[4,5], electrolytes[6], cholesterol[7,8], and for label-free monitoring of biomolecular interactions[9].

Recent measurements of liquid crystal monolayers on aqueous electrolytes have revealed that certain electrolytes shift the surface pressure-area isotherm such that the surface pressure increases either more rapidly or more slowly than for a pure water subphase during compression. Carlton *et al.*[10] showed that the orientation of 5CB liquid crystal in a monolayer can be modified in different electrolytes. It is useful to divide ions into chaotropic, which are typically large and weakly hydrated, and kosmotropic, which are typically smaller and more strongly hydrated, following the Hofmeister series[11]. Chaotropic ions such as iodide, perchlorate, and thiocyanate induce continuous orientation transitions from planar to homeotropic of the 5CB director. Kosmotropic ions, such as chloride and bromide, do not perturb the orientation of the 5CB away from planar when compared to a monolayer on pure water. Surface pressure-area isotherms also showed that

[a] *H.H. Wills Physics Laboratory, Tyndall Avenue, Bristol, BS8 1TL, UK; E-mail: j.hallett@bristol.ac.uk*
[b] *School of Chemistry, University of Bristol, Cantock's Close, Bristol, BS8 1TS, UK*
[c] *Centre for Nanoscience and Quantum Information, Tyndall Avenue, Bristol, BS8 1FD, UK*
[d] *Diamond Light Source, Harwell Science and Innovation Campus, Fermi Avenue, Didcot, OX11 0DE, UK*

† Electronic Supplementary Information (ESI) available: [details of any supplementary information available should be included here]. See DOI: 10.1039/b000000x/

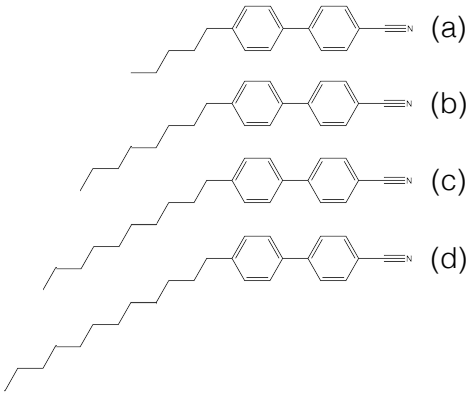

Fig. 1 Molecular structure of cyanobiphenyl homologues used in this study: a) 5CB, b) 8CB c) 10CB and d) 12CB.

chaotropic ions stabilise monolayers to higher areal densities and pressures than those for pure water or for kosmotropic ions. The increasing tendency of ions further along the Hofmeister series to disrupt ordering at amphiphile-aqueous interfaces is well-known from measurement of surface pressure-area isotherms[12,13], but the birefringent nature of liquid crystals also produces an optical indication of this interaction.

The structure of cyanobiphenyl liquid crystal monolayers has previously been studied via measurement of the surface pressure-area isotherms[2], optical second-harmonic generation[14] and Brewster Angle microscopy[15]. These measurements reveal that on pure water, *n*CBs form well-ordered thin films. In general, increasing the surface pressure causes the areal density to increase. However, when compressed beyond a certain point, the areal density can only increase further by reducing the number of molecules in the monolayer. It has been proposed that these molecules assemble into circular bilayer domains supported by the original monolayer, forming a "trilayer" structure. Support for this structure includes a constant surface pressure on compression beyond surface areas too small to accomodate all of the (insoluble) molecules at the water interface, a shift in the optical second-harmonic generation signal[14], and bright coalescing circular regions detected via Brewster angle microscopy at these areal densities[2].

Liquid crystal monolayers on pure water have also been studied using neutron reflectivity. Dent *et al.*[16] studied the cyanoterphenyl liquid crystal T15 and measured a surface pressure-area isotherm qualitatively similar to those reported for cyanobiphenyls[2,10,14]. However, they attributed the phase transitions in the isotherm slightly differently — due to the stronger tendency for cyanoterphenyl liquid crystals to form dimers — describing a monolayer - dimer monolayer - dimer bilayer - multilayer series on compression, supported by their neutron reflectivity data.

X-ray and Neutron reflectivity measurements have been widely performed on other monolayer forming systems on aqueous electrolyte subphases. The effective scattering length density of different components can be varied with both techniques, allowing for greater structural discrimination. Neutron reflectivity contrast can be modified for the aqueous subphase[17] by changing the ratio of hydrogenated and deuterated water, while the amphiphile contrast can also be varied through deuteration. X-ray reflectivity (XRR) is sensitive to effective electron density, so amphiphiles can be labelled with heavy atoms to increase contrast[18]. More generally X-ray reflectivity can also be used to detect ion localisation at interfaces[19–22]. The sensitivity to electron density for X-rays also means that contrast can also be modified by changing the X-ray energy. Vaknin *et al.*[23] used anomalous X-ray scattering to study the interaction between barium ions and biomimetic lipid membranes. The effective electron density of barium significantly varies at and away from the Ba L_{III} absorption edge (E = 5.247 keV) with a corresponding change to the reflectivity data. This approach confirmed the localisation of barium ions in a Stern layer, in addition to a diffuse component corresponding to the Debye-Hückel layer in solution. Further measurements have been used to study the interaction between bromide and monolayers of fatty acid[24] and caesium ions with lipid phosphate[25,26]. Another method to study the localisation of ions at charged Langmuir monolayers is X-ray fluorescence spectroscopy[27,28]. This can be used to identify localised enhancement of ions of a particular species, yielding information on their local environment[29].

In this exploratory work the monolayer structure of a series of cyanobiphenyl homologues supported on aqueous electrolyte subphases was studied using X-ray reflectivity. XRR represents an ideal tool to determine the presence of ions in a liquid crystal monolayer because the structure of the monolayer is revealed in addition to the ion distribution at the interface. Sodium bromide and sodium iodide were chosen as example kosmotropic and chaotropic ion systems respectively, due to their relatively large electron density over other salts in the Hofmeister series, giving them good X-ray contrast. The liquid crystals 5CB (figure 1a) and 8CB (figure 1b), widely used in the study of liquid crystal-aqeuous interfaces[2,6,10,14,15], were also studied here. The behaviour of 10CB (figure 1c) and 12CB (figure 1d) was also investigated to determine the effect of increasing alkyl tail length on monolayer structure.

2 Methods

Liquid crystal *n*CB homologues were purchased from Sigma Aldrich (8CB), Kingston Chemicals (5CB) and Synthon (10CB, 12CB). Monolayers were spread from *n*CB solutions in chloroform on water, 250 mM sodium bromide (Sigma, NaBr) and 250 mM sodium iodide (Sigma, NaI) aqueous salt solutions. Surface pressure-area isotherms and X-ray reflectivity were both measured on the monolayer systems in an enclosed teflon Langmuir trough (KSV Nima) kept under helium-rich atmosphere. XRR measurements were performed at the I07 beamline at the Diamond Light Source (Didcot, Oxfordshire) using the "Double Crystal Deflector" (DCD)[30,31] for reflectivity at liquid interfaces with X-ray energy 12.5 keV. Data was collected using a a Pilatus 100K detector. Specular reflection was integrated within a region of interest and a background region of the same size was subtracted. Data was collected over five attenuation regimes and normalized to the critical edge. To minimize beam damage the trough was translated between each run. Normalized XRR curves were fitted using the Motofit package[32] using a slab model. Each layer was

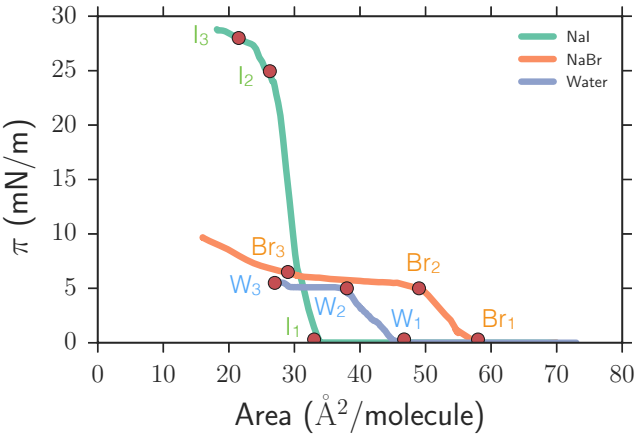

Fig. 2 Surface pressure-area isotherms for 8CB on NaI, NaBr and water subphases. Labelled red points indicate positions on isotherms where X-ray reflectivity data was taken.

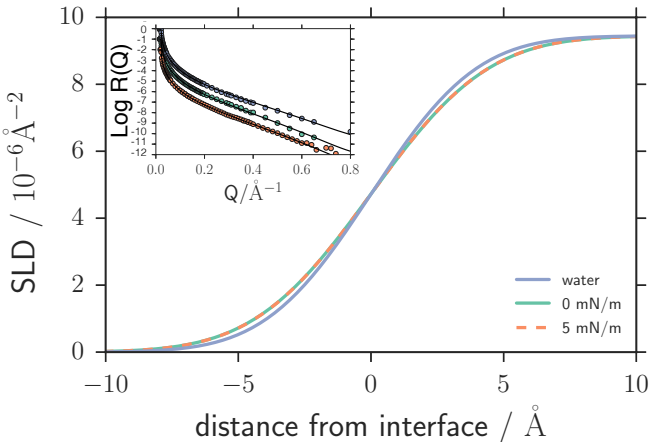

Fig. 3 Scattering length density profile and reflectivity data (inset) for pure water, and for 8CB supported on water at point 0 mN/m (W_1) and 5 mN/m (W_2). Reflectivity curves are offset for clarity.

defined by its scattering length density (which is directly proportional to electron density), its thickness and its roughness in order to specify the overall profile of the model. Typically the surface was well described by a two layer model — one predominately cyanobiphenyl and one ion rich. Additional layers were inserted until no improvement on fit refinement was obtained. Liquid crystal molecule lengths were determined using the software package Avogadro[33].

3 Results

3.1 Surface pressure-area isotherms

Isotherms for 5CB and 8CB were found to be in good agreement with previous measurements (Figure 2)[10]. At low areal densities, the surface pressure was zero, commonly interpreted as the *n*CB molecules forming isolated domains[14]. At approximately 45 Å^2 per molecule for the water subphase, these liquid domains coalesced into a continuous monolayer. Compressing further forced the molecules to adopt a more vertical orientation until the surface pressure reached a plateau at $\sim$ 5 mN/m. This plateau region has been attributed to the formation of a supported bilayer, or trilayer structure, as further compression acts to squeeze molecules out of the monolayer[2,14]. Similar behaviour was observed for the sodium bromide subphase, although the phase transitions were shifted to lower areal densities. For sodium iodide there was no plateau region and the monolayer was very stable with respect to compression, reaching surface pressures in excess of 25 mN/m. X-ray reflectivity data was generally measured at three points on each isotherm: where the pressure first increased from zero (point 1), at the beginning of the first plateau region (i.e. for a compressed monolayer) (point 2) and at maximum compression (or the point at which the plateau region began to further increase) (point 3). These points are labelled in figure 2 according to their subphases (e.g. point 1 for sodium bromide is labelled Br_1).

3.2 X-ray reflectivity from monolayers on a water subphase

X-ray reflectivity measurements of 5CB, 8CB, 10CB and 12CB liquid crystal on pure water were measured. The roughness of a pure water interface was measured to be 3.0 $\pm$ 0.3 Å, close to values reported previously[34].

Unlike the equivalent measurements with neutron reflectivity, where deuteration could be used to enhance contrast of the monolayer[16], spreading the liquid crystal on pure water produced little discernible change in the X-ray reflectivity (figure 3) at points W1 and W2 (figure 2) because the effective scattering length densities of *n*CBs ($\sim 9.3 \times 10^{-6}$ Å^{-2}) at 12.5 keV (calculated[35] from literature density values[36–39]) are very similar to that of water (9.47×10^{-6} Å^{-2}). A fit to the data for 8CB corresponded to a rough interface with a small increase in roughness beyond the water background at the interface, but with little change with increasing pressure. For both W1 and W2 (where the pressure initially increased from 0 mN/m and the beginning of the plateau region) the fitted surface roughness was 3.5 $\pm$ 0.4 Å.

The change in roughness between the monolayer and pure water system can be attributed to two possible sources. The roughness could be related to the reflectivity contribution of the liquid crystal monolayer, acting to smear out the interface slightly. Alternatively the change in roughness could be due to the change in surface tension of the water surface induced by the liquid crystal monolayer[40]. However, given that the increase in surface roughness was still detected for the monolayer with a surface pressure of 0 mN/m, the origin of the apparent increase in surface roughness can be attributed to the reflectivity contribution from the *n*CB molecules.

3.3 X-ray reflectivity from monolayers on a sodium iodide subphase

By changing the subphase to a 250 mN NaI solution, the X-ray reflectivity and surface pressure-area isotherm (figure 2) were dra-

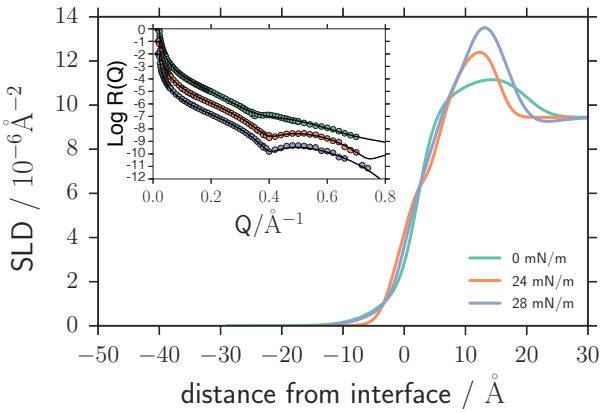

Fig. 4 Scattering length density distribution and reflectivity (inset) for 8CB supported on 250 mM NaI at ∼ 0 mN/m (point I_1), 24 mN/m (point I_2) and 28 mN/m (point I_3) surface pressures. Reflectivity curves are offset for clarity.

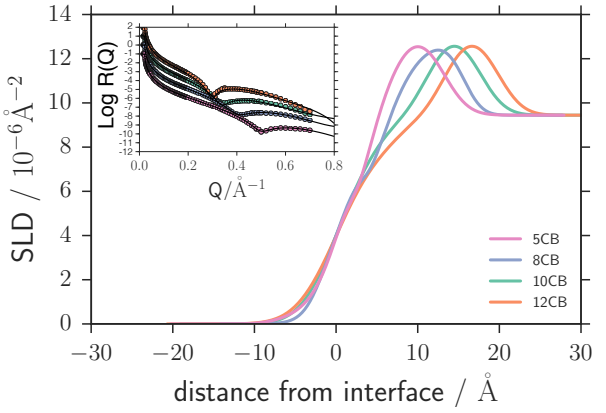

Fig. 5 Scattering length density distribution and reflectivity (inset) for 5CB, 8CB, 10CB and 12CB compressed monolayers spread on 250 mM NaI at ∼ 24 mN/m surface pressure (point I_2). Reflectivity curves are offset for clarity.

matically altered from the case of pure water for all *n*CBs. For 8CB at low surface pressure, the reflectivity data could be fitted with a broad peak in scattering length density above the level of the water subphase close to a rough interface (figure 4). This peak could be attributed to iodide ions forming a closely bound Stern layer and either a more diffuse Debye layer, or broadening due to variation in the monolayer thickness. At higher areal densities the distribution of the iodide peak narrowed, which indicates that the 8CB molecules are being compressed into a more densely packed, highly ordered homeotropic layer and the localisation of the iodide ions is increasing at the interface (illustrated in figure 8a). These results are consistent with the optical tilt angle measurements reported previously at a bulk liquid crystal - aqueous interface [10].

Similar behaviour was found for the full series of liquid crystal homologues, with the iodide peak moving further from the air interface as the layer thickness increased with increasing alkyl chain length. Figure 5 shows the reflectivity and scattering length density distribution for each homologue in the series in a compressed monolayer (i.e., at point I_2 in the isotherm).

Figure 6 shows the fitted layer thickness from the air interface to the iodide peak, and the all-*trans* molecule length, for increasing alkyl chain length. The thickness of the hydrocarbon layer increases with *n*, the number of carbons in the alkyl tail in *n*CB. This increase in layer thickness between each *n*CB scales linearly with the alkyl tail length, consistent with a common orientation for all the liquid crystal species supported on sodium iodide. The gradient indicates that the layer thickness increased by 1.21 ± 0.05 Å per carbon atom in the alkyl chain. By modelling the cyanobiphenyl homologues and obtaining their dimensions, the increase in molecule length per carbon atom in the alkyl tail can also be determined. This gives a value of 1.255 ± 0.011 Å per carbon atom for the all-*trans* length of the molecules, only slightly larger than the experimental value determined from fitting the X-ray reflectivity. This indicates that that the molecules in the monolayer have a tilt of approximately 16° from vertical at the interface, consistent with the tilt expected from surface-area arguments for a compressed film [10]. However, the intercept of 6.37 ± 0.46 Å determined for the fitted layer thicknesses is rather less than the 9.40 Å expected for the cyanobiphenyl group (or equivalently, a 0CB molecule) at the same orientation. This indicates that, although the cyanobiphenyl remains roughly perpendicular to the surface at this part of the isotherm, the cyano group and part of the first phenyl ring are embedded in the aqueous phase alongside the iodide ions. This is consistent with the observations of Zhang *et al.* [41], who, using sum frequency generation vibrational spectroscopy, detected penetration of water molecules between the cyano groups of 5CB and 8CB monolayers, but not for 5CT (terphenyl). They attributed this to the greater attraction between terphenyl groups than biphenyl groups preventing water penetration. Recent simulation work [42] also showed that the free energy is minimised for 5CB at the water-liquid crystal interface when the cyano group and part of the first phenyl ring are hydrated.

By integrating the iodide peak in the scattering length density profile for each *n*CB monolayer (above the water subphase scattering length density), the areal density of iodide ions can be determined (see appendix A). For the *n*CB homologous series the area per iodide ion was determined to be ≈ 34 ± 7 Å^2, close to the ∼ 30 Å^2 per *n*CB molecule in the monolayers. This strongly suggests that an iodide ion tends to localise at the cyano group for each cyanobiphenyl molecule in the compressed monolayer, indicating that the formation of a Stern layer stabilises the film to higher areal densities than for monolayers on pure water.

3.4 X-ray reflectivity from monolayers on a sodium bromide subphase

In this section, the phase behaviour and structure of *n*CB liquid crystal monolayers supported by sodium bromide solutions are considered. Unlike for NaI, at low *n*CB areal density, there was little enhancement of the XRR (and so, the scattering length density) beyond that of the liquid crystal on pure water. This suggests

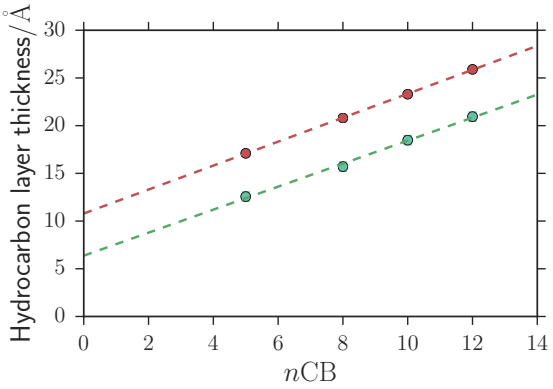

Fig. 6 Hydrocarbon layer thickness as a function of alkyl chain length for 5CB, 8CB, 10CB and 12CB supported on 250 mM NaI at ∼ 24 mN/m surface pressure. Green points are experimental values, red points are all-*trans* molecular lengths.

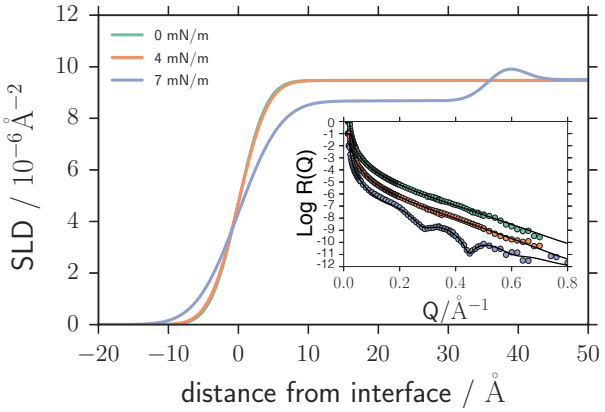

Fig. 7 Scattering length density distribution and reflectivity (inset) for 8CB supported on 250 mM NaBr at 0 mN/m (point Br_1), 4mN/m (point Br_2) and 7 mN/m (point Br_3). Distances taken relative to air interface. Reflectivity curves are offset for clarity.

that no tightly bound Stern layer of bromide ions was formed close to the liquid crystal cyano headgroup (figure 7) for all *n*CB species. At these low surface pressures (points Br_1 and Br_2), there were no features in the reflectivity data and no discernible peak in the scattering length density. At these pressures it is therefore not possible to estimate the layer thickness. However, it should be noted that bromide localisation would not be clearly detected if the layers of liquid crystal and ions were thin enough such that any features in the reflectivity data were beyond $Q_{max} = 0.8$ Å^{-1}.

For 5CB and 8CB, some features emerged in the X-ray reflectivity data with increasing areal density, specifically on the trilayer region of the surface pressure-area isotherm (i.e. between points Br_2 and Br_3 - see figure 2). However, no change in the reflectivity data was detected for 10CB and 12CB with increasing areal density, and the surface pressure was observed to rapidly collapse to 0 mN/m, indicating that their monolayers were unstable on sodium bromide, tending to form multilayers spontaneously at low compression. Fits to the reflectivity data for 8CB indicated the presence of a peak in scattering length density 40 Å from the air interface at a surface pressure of 7 mN/m (point Br_3). At point Br_3 this peak became quite significant, reaching a maximum value 0.50×10^{-6}Å^{-2} above the water background. This spacing of 40 Å is sufficient to account for the thickness of the 8CB bilayer (measured to be 31.6 Å in bulk 8CB[43,44]) with the remaining ∼ 8.4 Å accounting for the planar oriented (partially solvated) 8CB molecule at the aqueous interface. Xue *et al.*[14] reported that the 8CB in contact with water has a tilt angle of 68.5°. Taking the 8CB molecule length to be 20.8 Å, this gives a layer thickness of 7.6 Å. Although this is slightly lower than the ∼ 8.4 Å reported here, it is also possible that in the trilayer the interfacial 8CB molecules are less tilted than in the monolayer. Closer to the air interface the fitted scattering length density was lower than that for pure water, which is also consistent with liquid crystal trilayer domain formation rather than a continuous layer, which would have a scattering length density close to that of water. The ratio of SLD between this region and bulk *n*CB suggests coverage of approximately 90%, consistent with the amount observed using Brewster-Angle microscopy[2] at the equivalent state point on water. Therefore the trilayer structure, previously interpreted from surface pressure-area isotherms and Brewster-Angle microscopy[15], has been measured directly here.

As for the sodium iodide system, by integrating the scattering length density of the peak above the water background, the areal density of bromide ions was determined from the 7 mN/m data, giving a value of 114 Å^2 per bromide ion, significantly greater than the ∼ 30 Å^2 per *n*CB molecule. We interpret this to mean that the *n*CB molecules in contact with the water are lying flat and supporting a ∼ 31.6 Å thick bilayer as indicated in the SLD distribution resulting from the fit (figure 7).

It is surprising that the localisation of bromide ions at the *n*CB interface can only be detected for compressed films. By taking the layer thickness of the *n*CB monolayer to be 8 - 12 Å (from surface area arguments and assuming some hydration of the cyano group, as in the iodide case), and similar bromide density as for the trilayer case, some deviations should still be detected at high *Q* if the bromide ions are indeed localising at the interface. The effect of bromide on the behaviour of the film can be rationalised as follows. The bromide ions increase the area occupied by each molecule which lie flat in the "rafts" at high mean area per molecule. No bound layer is detected, which implies that the Br remains in a diffuse layer and the increase in molecular area must be an ionic atmosphere effect (figure 8b). This increased area occupied by each molecule results in the rafts fusing at a higher mean area per molecule and so the surface pressure increases from zero at a higher mean area per molecule compared to the pure water case. As the compression is increased, the molecules begin to tilt and the pressure rises. When the pressure is about 5 mN/m the transition to a trilayer begins. The trilayer structure further stabilises the tilt of the molecules and, with the cyano groups pointing more into the water (increasing the availability of cyano groups to bromide), a Stern layer of bound bromide ions is formed (figure 8c).

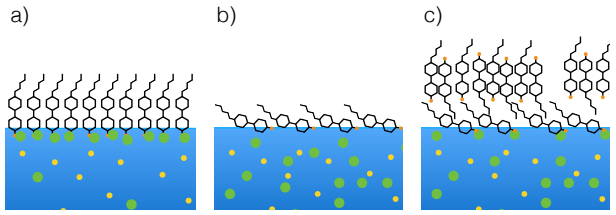

Fig. 8 Schematic illustration of 5CB liquid crystal supported on a) sodium iodide, b) sodium bromide (low pressure) and c) sodium bromide (high pressure). Yellow circles represent sodium ions. Green circles represent halide ions.

4 Conclusions

The structure and phase behaviour of cyanobiphenyl liquid crystal monolayers supported on aqueous electrolyte subphases was studied. Measurements to date on this family of systems principally rely on the change in polarising microscopy signal generated by the reorientation of birefringent liquid crystal, or from changes in the surface pressure-area isotherm, to infer structural changes in the liquid crystal layer. Here, for the first time, X-ray reflectivity was applied to liquid crystal-aqueous electrolyte interfaces to study both the liquid crystal monolayer structure, and the complimentary structure of the ionic species in the aqueous phase.

For a liquid crystal monolayer, rather than a nematic bulk, weakly hydrated, chaotropic ions such as sodium iodide stabilise the monolayer to higher areal densities, i.e. they promote alignment more perpendicular to the aqueous surface than for pure water. X-ray reflectivity shows that the cyanobiphenyl molecules become vertically oriented and a Stern layer of bound ions forms with the cyano group, similar to the case of lipids and surfactants on electrolyte solutions[23,45,46]. The increase of the layer thickness with alkyl chain length indicates that these molecules are nearly vertically oriented, and that the cyano headgroup penetrates into the aqueous phase where it binds with the iodide ions. The areal density of the iodide ions, determined from the peak in the scattering length density from fitting the X-ray reflectivity with a slab model, is close to that of the liquid crystal areal density, implying a one-to-one binding of ion to headgroup. This binding could occur through a dipole - induced dipole interaction between each liquid crystal cyano group, which posesses a large dipole moment, and an iodide ion, which is relatively large and polarisable[10]. It was observed that this cyano-iodide interaction is sufficient to stabilise all of the *n*CB monolayers studied here (5CB-12CB), including those which are otherwise unstable to monolayer compression on pure water (10CB and 12CB).

Unlike sodium iodide, sodium bromide does not stabilise liquid crystal monolayers to higher areal densities than pure water. Instead, the surface pressure increases more rapidly than even for pure water before reaching a plateau in surface pressure, previously attributed to the formation of a trilayer structure, where bilayer domains are supported on the monolayer. X-ray reflectivity measurements reveal that at low areal density, there is no localisation of ions at the water interface. However, for higher areal densities a Stern layer of bromide ions emerges ~ 40 Å from the air interface, and the scattering length density of this region is markedly lower than that of water. This observation is consistent with the formation of trilayer domains, and provides a direct measurement of the thickness of these regions. This behaviour was observed for 5CB and 8CB, but not 10CB and 12CB, which were unstable to compression on sodium bromide.

Liquid crystal - aqueous interfaces are cited as an ideal candidate for low cost, high sensitivity chemical sensors. Recent measurements have shown that specific ion-induced surface reorientations can propagate and align a bulk nematic phase, creating an optical signal in the presence of specific chemicals. The interaction between ions, liquid crystal and other dopants has been proposed as a detection vector for systems as diverse as ion-DNA complex assays[47], and mercury ion detection in drinking water[48]. This study highlights some of the features of these interactions, which could help guide the design of liquid crystal interface-based lab-on-a-chip devices. Future work will extend this study to neutron reflectivity, where contrast can be improved between *n*CB and water through deuteration. This will improve structural discrimination for the monolayer systems which had little X-ray contrast here.

5 Acknowledgements

JEH and DW were supported by EPSRC CDT grant EP/G036780/1. The authors thank Diamond Light source for provision of beamtime (experiment number SI11363).

6 Appendix A: Calculation of adsorbed layer density

The amount of halide ions absorbed at the interface between the solution and the cyanobiphenyl film can be estimated as follows[19]: The scattering length density profile $\rho(z)$ determined by the number of electrons in each species (a_i where $i = H_2O$, Ha or CB for water molecules, halide ions or cyanobiphenyl molecules) and the number density (n_i) of each species:

$$\rho(z) = r_e\left[n_{\mathrm{CB}}(z)a_{\mathrm{CB}} + n_{\mathrm{Ha}}(z)a_{\mathrm{Ha}} + n_{\mathrm{H_2O}}(z)a_{\mathrm{H_2O}}\right] \quad (1)$$

where z is the distance perpendicular to the air interface and r_e is the Thompson scattering lengths of one electron. In the halide-rich region, the number density of water molecules is less than that of of pure water because of the volume occupied by the halide ions:

$$\rho(z) = r_e\left[n^0_{\mathrm{CB}}(z)a_{\mathrm{CB}} + n_{\mathrm{Ha}}(z)\left(a_{\mathrm{Ha}} - \frac{v_{\mathrm{Ha}}}{v_{\mathrm{H_2O}}}a_{\mathrm{H_2O}}\right) + n^0_{\mathrm{H_2O}}(z)a_{\mathrm{H_2O}}\right] \quad (2)$$

where v_i is the partial molar volume of species i in dilute aqueous solution. $n^0_i(z)$ is used to indicate the constant number density of the species in the pure bulk media, falling rapidly to zero at the aqueous - cyanobiphenyl interface.

In this system, the scattering length densities the cyanobiphenyl and the aqueous phases are very close (see table 1). Thus there is a peak in the scattering length density profile due to the halide rich layer, which has a higher SLD than both pure cyanobiphenyl and pure water. Its area A may be calcuated by subtracting the SLD profile of the pure water and

cyanobiphenyl ρ^0 meeting at the interface, and integrating over z to get the number halide of ions per unit area Γ_{Ha}.

$$\rho^0(z) = r_e \left[n^0_{\mathrm{CB}}(z) a_{\mathrm{CB}} + n^0_{\mathrm{H_2O}}(z) a_{\mathrm{H_2O}} \right] \tag{3}$$

$$A = \int \left(\rho(z) - \rho^0(z) \right) dz = r_e \left[\Gamma_{\mathrm{Ha}} \left(a_{\mathrm{Ha}} - \frac{v_{\mathrm{Ha}}}{v_{\mathrm{H_2O}}} a_{\mathrm{H_2O}} \right) \right] \tag{4}$$

Therefore the area per halide ion is simply the inverse $\Gamma^{-1}_{\mathrm{Ha}}$:

$$\Gamma^{-1}_{\mathrm{Ha}} = \frac{r_e \left(a_{\mathrm{Ha}} - \frac{v_{\mathrm{Ha}}}{v_{\mathrm{H_2O}}} a_{\mathrm{H_2O}} \right)}{A} \tag{5}$$

The main error in this approach is the accuracy of extrapolating and subtracting the SLD of the aqueous phase and the cyanobiphenyl. Table 1 shows an example of this calculation for iodide and bromide ions.

References

1 L. M. Blinov, *Structure and properties of liquid crystals*, Springer, 2010.

2 M. N. G. de Mul and J. A. Mann, *Langmuir*, 1994, **10**, 2311–2316.

3 R. J. Carlton, J. T. Hunter, D. S. Miller, R. Abbasi, P. C. Mushenheim, L. N. Tan and N. L. Abbott, *Liquid crystals reviews*, 2013, **1**, 29–51.

4 I.-H. Lin, D. S. Miller, P. J. Bertics, C. J. Murphy, J. J. De Pablo and N. L. Abbott, *Science*, 2011, **332**, 1297–1300.

5 D. S. Miller and N. L. Abbott, *Soft Matter*, 2013, **9**, 374–382.

6 R. J. Carlton, J. K. Gupta, C. L. Swift and N. L. Abbott, *Langmuir*, 2011, **28**, 31–36.

7 M. Tyagi, A. Chandran, T. Joshi, J. Prakash, V. Agrawal and A. Biradar, *Applied Physics Letters*, 2014, **104**, 154104.

8 Y. Wei and C.-H. Jang, *Journal of Materials Science*, 2015, **50**, 4741–4748.

9 J. M. Brake, M. K. Daschner, Y.-Y. Luk and N. L. Abbott, *Science*, 2003, **302**, 2094–2097.

10 R. J. Carlton, C. D. Ma, J. K. Gupta and N. L. Abbott, *Langmuir*, 2012, **28**, 12796–12805.

11 W. Kunz, *Current Opinion in Colloid & Interface Science*, 2010, **15**, 34–39.

12 M. C. Gurau, S.-M. Lim, E. T. Castellana, F. Albertorio, S. Kataoka and P. S. Cremer, *Journal of the American Chemical Society*, 2004, **126**, 10522–10523.

13 A. Aroti, E. Leontidis, E. Maltseva and G. Brezesinski, *The Journal of Physical Chemistry B*, 2004, **108**, 15238–15245.

14 J. Xue, C. S. Jung and M. W. Kim, *Physical Review Letters*, 1992, **69**, 474–477.

15 M. N. G. de Mul and J. A. Mann, *Langmuir*, 1998, 2455–2466.

16 N. Dent, M. Grundy, R. Richardson, S. J. Roser, N. McKeown and M. Cook, *Journal de Chimie Physique et de Physico-Chimie Biologique*, 1988, **85**, 1003–1008.

17 R. Richardson and S. Roser, *Langmuir*, 1991, **7**, 1458–1467.

18 U. Rost, Y. Xu, T. Salditt and U. Diederichsen, *ChemPhysChem*, 2016, **17**, 2525–2534.

19 R. Richardson and S. Roser, *Liquid Crystals*, 1987, **2**, 797–814.

20 M. Grundy, R. Richardson, S. Roser, J. Penfold and R. Ward, *Thin Solid Films*, 1988, **159**, 43–52.

21 I. Weissbuch, R. Buller, K. Kjaer, J. Als-Nielsen, L. Leiserowitz and M. Lahav, *Colloids and Surfaces A: Physicochemical and Engineering Aspects*, 2002, **208**, 3–27.

22 G. Luo, W. Bu, M. Mihaylov, I. Kuzmenko, M. L. Schlossman and L. Soderholm, *Journal of Physical Chemistry C*, 2013, **117**, 19082–19090.

23 D. Vaknin, P. Krüger and M. Lösche, *Physical review letters*, 2003, **90**, 178102.

24 J. Strzalka, E. DiMasi, I. Kuzmenko, T. Gog and J. K. Blasie, *Physical Review E*, 2004, **70**, —-051603.

25 W. Bu, D. Vaknin and A. Travesset, *Physical Review E*, 2005, **72**, 8–11.

26 W. Bu, D. Vaknin and A. Travesset, *Langmuir*, 2006, **22**, 5673–5681.

27 W. B. Yun and J. M. Bloch, *Journal of Applied Physics*, 1990, **68**, 1421–1428.

28 J. Bloch, M. Sansone, F. Rondelez, D. Peiffer, P. Pincus, M. Kim and P. Eisenberger, 1985, **54**, 1039–1042.

29 W. Bu and D. Vaknin, *Journal of Applied Physics*, 2009, **105**, year.

30 C. Nicklin, T. Arnold, J. Rawle and A. Warne, *Journal of Synchrotron Radiation*, 2016, **23**, year.

31 T. Arnold, C. Nicklin, J. Rawle, J. Sutter, T. Bates, B. Nutter, G. McIntyre and M. Burt, *Journal of synchrotron radiation*, 2012, **19**, 408–416.

32 A. Nelson, *Journal of Applied Crystallography*, 2006, **39**, 273–276.

33 M. D. Hanwell, D. E. Curtis, D. C. Lonie, T. Vandermeersch, E. Zurek and G. R. Hutchison, *Journal of cheminformatics*, 2012, **4**, 17.

34 P. S. Pershan, *Faraday Discuss. Chem. Soc.*, 1990, **89**, 231–245.

35 R. M. Richardson, *Colloid science: principles, methods and applications*, John Wiley & Sons, 2010, ch. 13, pp. 273–298.

36 I. Zgura, R. Moldovan and T. Beica, *Crystal Research and Technology*, 2009, **44**, 883–888.

37 I. Cacelli, L. De Gaetani, G. Prampolini and A. Tani, *The Journal of Physical Chemistry B*, 2007, **111**, 2130–2137.

38 A. Leadbetter, J. Durrant and M. Rugman, *Molecular Crystals and Liquid Crystals*, 1976, **34**, 231–235.

39 V. Raja, S. K. Prasad, D. S. Rao and S. Chandrasekhar, *Liquid Crystals*, 1992, **12**, 239–243.

40 G. J. Simpson and K. L. Rowlen, *Chemical physics letters*, 1999, **309**, 117–122.

41 Z. Zhang, D.-S. Zheng, Y. Guo and H.-F. Wang, *Physical chemistry chemical physics : PCCP*, 2009, **11**, 991–1002.

42 H. Ramezani-Dakhel, M. Sadati, M. Rahimi, A. Ramirez-Hernandez, B. Roux and J. J. de Pablo, *Journal of Chemical Theory and Computation*, 2016, **13**, 237–244.

43 M. Fukuto, O. Gang, K. J. Alvine, B. M. Ocko and P. S. Pershan,

Table 1 Table of example values used to determine ion layer densities in liquid crystal monolayers.

Species	a	ν/cm^3	$\rho/(10^{-6}\ \text{Å}^{-2})$	$A/(10^{-6}\ \text{Å}^{-1})$	$\Gamma/(\text{Å}^{-2})$	$\Gamma^{-1}/(\text{Å}^2)$
I^-	54	41.6	-	35	0.0390	25
Br^-	36	30.1	-	4.8	0.0087	114
H_2O	10	18	9.53	-	-	-
8CB	158	294	9.22	-	-	-

Physical Review E, 2008, **77**, 031607.

44 M. Sadati, H. Ramezani-Dakhel, W. Bu, E. Sevgen, Z. Liang, C. Erol, M. Rahimi, N. Taheri Qazvini, B. Lin, N. L. Abbott *et al.*, *Journal of the American Chemical Society*, 2017, **139**, 3841–3850.

45 J. Pittler, W. Bu, D. Vaknin, A. Travesset, D. McGillivray and M. Lösche, *Physical review letters*, 2006, **97**, 046102.

46 W. Wang, R. Y. Park, A. Travesset and D. Vaknin, *Physical review letters*, 2011, **106**, 056102.

47 Y. Liu and K.-L. Yang, *Journal of colloid and interface science*, 2015, **439**, 149–153.

48 S. K. Singh, R. Nandi, K. Mishra, H. K. Singh, R. K. Singh and B. Singh, *Sensors and Actuators B: Chemical*, 2016, **226**, 381–387.